JOURNAL OF CATALYSIS **174,** 153–163 (1998)
ARTICLE NO. CA971965

The Characterization of BaF_2/Y_2O_3 Catalysts for the OCM Reaction

C. T. Au,[1] X. P. Zhou,[2] Y. W. Liu, W. J. Ji,[3] and C. F. Ng

Department of Chemistry and Centre for Surface Analysis and Research, Hong Kong Baptist University, Kowloon Tong, Hong Kong, China

Received July 11, 1997; revised November 7, 1997; accepted November 11, 1997

The reactivities of Y_2O_3 and BaF_2/Y_2O_3 catalysts have been investigated for the oxidative coupling of methane (OCM) reactions. With $CH_4:O_2:N_2 = 2.47:1:11.4$ and a total flow rate of 50 mL min^{-1}, after 4 h of reaction time at 750°C, the CH_4 conversion and C_2 selectivity over Y_2O_3 were 29.9 and 26.2%, respectively, giving a C_2 yield of 7.8%. When 30 mol% of BaF_2 was added, the CH_4 conversion, C_2 selectivity, and C_2 yield were enhanced to 35.3, 55.4, and 19.5%, respectively. With a 95 mol% BaF_2/Y_2O_3 catalyst, we could achieve a 22.4% C_2 yield with CH_4 conversion and C_2 selectivity, respectively, equal to 36.1 and 62.1%. X-ray diffraction (XRD) investigation of the BaF_2/Y_2O_3 catalysts revealed that the cubic Y_2O_3 lattice had expanded slightly while the cubic BaF_2 phase contracted. Based on the results of O_2 absorption as well as temperature-programmed reduction (TPR) studies, we know that the BaF_2/Y_2O_3 catalysts have higher ability in O_2 activation than the undoped Y_2O_3 catalyst. We suggest that the ionic exchange which occurred between the BaF_2 and Y_2O_3 phases caused the generation of active defects. We used the EPR technique to monitor the generation of trapped electrons in the 95 mol% BaF_2/Y_2O_3 catalyst. The results indicated that there were reducible oxygen ions which existed largely in the bulk. After H_2 reduction between 500 and 700°C, a kind of trapped electron with EPR signal centered at 2.0871 was formed. H_2 reduction above 700°C could result in the generation of another type of trapped electron with EPR signal centered at 2.0087. The 2.0871 signal showed doublet superhyperfine structures while the 2.0087 one was symmetrical. We interpret the former as being due to trapped electrons interacting with the Y^{3+} ions, while the latter due to trapped electrons shared among the orbitals of the surrounding cations. The 2.0871 trapped electrons spread throughout the sample, while the 2.0087 ones existed only on the surface. The involvement of surface-trapped electrons in activating O_2 was observed at 25°C, while above 500°C, trapped electrons in the bulk were also involved. According to the results obtained, we have reasons to believe that in the OCM reaction, the BaF_2/Y_2O_3 catalysts were reduced by hydrogen dissociated from methane, and trapped electrons were generated. These trapped electrons could serve as active sites for O_2 activation.

Key Words: **OCM reaction; BaF_2/Y_2O_3 catalysts; O_2 activation; trapped electrons.**

INTRODUCTION

The formation of oxygen species such as O^-, O_2^{2-}, O_2^-, and O_3^- on the surface of metal oxide catalysts has been reported frequently (1–6). The existence of these kinds of oxygen ions is important for the selective oxidation of alkanes. It is generally believed that there are electron-donor sites on the surface of the catalysts. When oxygen molecules receive electrons from these sites, oxygen ions such as O^- and O_2^- are formed. Although direct evidence is lacking, it has been accepted that one such donor site is the low-coordinated O^{2-} sites (7, 8). As reported by Wang and Lunsford (9), when Li/MgO was quenched from 650°C in O_2 atmosphere by liquid nitrogen, O^-, O_2^-, and O_3^- were detected. Under UV irradiation, Mg^+_{LC}–O^-_{LC} exciton was believed to form when a photon was absorbed at an anion site (10, 11). The electrons were trapped on Mg^+ ions and were very unstable. When UV light was cut off, such centers disappeared at once (7). In the presence of O_2, molecular oxygen could combine with these trapped electrons to form O_2^- ions, or combine with O^- to form O_3^- ions. Hydrogen heterolytical dissociation on a catalyst surface can also generate electron donors (12). It has been reported that oxygen molecules can obtain electrons from hydride ions to form O_2^- ions (13). These types of electron donors are not stable in the presence of O_2.

Osada *et al.* (14) studied the Y_2O_3–CaO catalysts for the OCM reaction. They found that with increasing Y_2O_3 content in the coprecipitated catalysts, the C_{2+} selectivity at 700°C was significantly enhanced. They attributed this to the formation of a solid solution accompanying the production of interstitial superoxide ions, O_2^-. They reported that the distortion of the Y_2O_3 lattice could affect the C_{2+} selectivity. In a paper on the characterization of Ba-doped yttria oxidative coupling catalyst by XANES (oxygen K-edge), Kaminsky *et al.* (15) proposed that as Ba^{2+} substituted into the Y^{3+} lattice sites, charge-deficient oxygen sites were created. Erarslanoglu *et al.* (16) reported the effect of Sr dopants on the catalytic performance of Y_2O_3 in the OCM reaction. They observed the incorporation of Sr^{2+} cations into the lattice structure of Y_2O_3. The CH_4 conversion and C_{2+} selectivities were substantially higher over the Sr/Y_2O_3 catalyst than over the undoped Y_2O_3

[1] To whom correspondence should be addressed.

[2] Present address: Symyx Technologies, 420, Oakmead Parkway, Sunnyvale, CA 94086.

[3] On leave from School of Chemistry and Chemical Engineering, Nanjing University, PR China.

0021-9797/98 $25.00

catalyst. In our earlier work (17), we reported the existence of trapped electrons in a 20% SrF_2/SmOF catalyst. We deduced that the EPR-detectable trapped electrons were located in the distorted SrF_2 phase. Unlike electron donors in metal oxides, these trapped electrons were stable and a large number of them were located in the bulk of SrF_2/SmOF. Only surface-trapped electrons would react with O_2 at 25°C. Above 300°C, trapped electrons in the bulk migrated to the surface and became involved in O_2 activation. We have now extended our studies to the BaF_2/Y_2O_3 system. We doped BaF_2 with 5 mol% of Y_2O_3. The use of 95 mol% of BaF_2 was to make available a F^- matrix in which the trapped electrons generated could be stabilized, whereas the employment of Y^{3+} ions (nuclear spin number, 1/2) was to provide us with a means of identifying the location(s) of the trapped electrons. We have also studied the combination of O_2 with trapped electrons as related to the activation of O_2 over the 95 mol% BaF_2/Y_2O_3 catalyst, which is active in the oxidative coupling of methane reactions.

EXPERIMENTAL

The BaF_2/Y_2O_3 catalysts were prepared by mixing Y_2O_3 (Aldrich, 99.99%) with BaF_2 (Beijing Chemicals, >99.7%) at the right molar ratios. The mixture was moistened with deionized water and was properly ground. After being dried at 200°C (6 h), the material was extruded to pellets at 300 kg cm^{-2} pressure and calcined in air at 800°C for 3 to 5 h. The solid was then crushed and sieved to 0.2–0.5 mm. The specific surface area of the catalyst was measured by the BET method. The continuous-flow chromatographic technique was adopted with helium as the carrier gas and nitrogen as the adsorbate.

The performances of the BaF_2/Y_2O_3 catalysts in the OCM reaction were examined in a flow system (18). The sample (0.5 g) was placed in a fixed bed (i.d. 5 mm) quartz microreactor. The feed for the OCM reaction was composed of CH_4, O_2, and N_2 in a 2.47 : 1 : 11.4 ratio. The total flow rate was 50 mL min^{-1}. The reaction products were analyzed by online gas chromatography (Shimazu GC-8A). A blank reactor showed no activity whatsoever below 800°C under these conditions. The calculations of methane conversion and selectivity for C_2 were based on total carbon balance. A carbon balance of 100 ± 1% was obtained for every run over the catalysts. The conversion of methane was defined as

$$c(CH_4) = \frac{\text{moles } CH_4 \text{ converted}}{\text{moles } CH_4 \text{ fed}} \times 100\%.$$

The selectivity for C_2 products was calculated as

$$s(C_2) = \frac{2 \times \text{moles } (C_2H_4 + C_2H_6) \text{ in products}}{\text{moles } CH_4 \text{ converted to all products}} \times 100\%.$$

The yield for C_2 product was given by

$$y(C_2) = c(CH_4) \times s(C_2).$$

For the analysis of F content, the F^- ion-electrode method was used. A calibration line of log [F^- ions concentration] versus the electrode voltage was first obtained. About 20 mg sample was dissolved in ca. 2 mL 6 *M* HNO_3 solution. Then the pH of the solution was adjusted to be between 6 and 7 using a 1.1 *M* CH_3COONa solution. Distilled water was added to the resulting solution to make up a volume of 50 mL. With the measurement of electrode voltage by a digital pH/millivolt meter 611 (Orion Research) combined fluoride ion selective electrode, the F^- ion concentration in the solution could be estimated against the calibration curve of standard NaF solutions.

XRD measurements were performed on a Rigaku Rotaflex D/Max-C system with CuK_α radiation. X-ray photoelectron spectroscopy (Leybold Heraeus-Shenyang SKL-12) was used to characterize the catalyst surface. The binding energies were calibrated to the C1*s* value (284.6 eV) of contaminant carbon. Surface compositions were calculated using the equation

$$X_i = (A_i/S_i) \times 100 \Big/ \sum (A_i/S_i),$$

where A_i is the peak area of XPS signal of element *i*, and S_i is the corresponding atomic sensitivity factor.

The EPR recordings were carried out on a Bruker ER-2000-SRC EPR spectrometer. Samples (1.515 g) after various treatments were examined in the X band at 25°C. The EPR system was equipped with a quartz-tube reactor which was transferable between the sample chamber and an oven. The sample in the quartz reactor could be heated to 900°C and exposed to reactant gas without being exposed to air. Raman experiments were performed over a Nicolet 560 FT Raman spectrometer. The samples were treated in O_2, N_2, H_2, and O_2 successively at different temperatures. After various treatments, the samples were monitored at 25°C without being exposed to air.

The O_2-pulse measurements were performed on a GC-MS (HP G1800A) system. The pulse size of the gases was 65.7 μL (at 25°C, 1 atm). The temperature-programmed reduction (TPR) experiments were conducted using a 7% H_2–93% N_2 (v/v) mixture. The flow rate was 50 mL min^{-1} and a thermal conductivity detector was used. Catalyst weight was 0.2 g and the heating rate was 10°C min^{-1}. The catalysts had been treated in O_2 at 800°C for 1 h and cooled to RT in O_2 before the TPR experiments were performed.

RESULTS

Catalytic Activities and BET Measurements

Table 1 shows the performances of the BaF_2/Y_2O_3 catalysts (readings were taken 1 h after temperature stabilization) as related to BaF_2 composition. One can see that

TABLE 1

The Catalytic Performances of BaF_2/Y_2O_3 Catalysts with Different BaF_2 Composition

BaF_2 composition (%)	T (°C)	Conversion (%)			Selectivity (%)			C_2 Yield (%)	Rate of CH_4 reaction (10^{18} molecules m^{-2} s^{-1})
		CH_4	O_2	CO_x	C_2H_4	C_2H_6	C_2		
0	600	25.0	89.0	88.5	4.8	6.7	11.5	3.00	0.16
	650	25.9	89.5	84.7	7.9	7.4	15.3	4.00	0.16
	700	26.8	91.5	79.1	13.3	7.6	20.9	5.60	0.17
	750	30.3	92.8	73.8	18.0	8.2	26.2	7.80	0.20
	800	31.8	92.0	73.1	16.3	8.6	26.9	8.60	0.21
10	600	17.2	64.8	77.6	7.20	15.2	22.4	3.90	0.031
	650	31.0	82.1	58.2	20.7	21.1	41.8	13.0	0.56
	700	33.0	93.3	51.1	25.0	24.9	48.9	16.2	0.60
	750	32.5	94.0	50.8	25.0	24.2	49.2	16.0	0.60
	800	29.4	95.1	56.9	26.1	17.1	43.1	12.7	0.53
30	650	12.9	64.4	79.1	6.30	14.6	20.9	2.70	0.30
	700	30.6	90.1	62.1	20.4	17.5	37.9	11.6	0.70
	750	38.2	92.4	53.4	29.9	16.7	46.6	17.8	0.87
	800	39.0	95.3	49.6	33.3	17.1	50.4	19.7	0.88
50	600	9.50	32.7	79.3	3.90	16.4	20.3	1.90	0.23
	650	27.9	79.3	58.3	18.6	23.1	41.7	11.7	0.67
	700	36.3	90.1	48.7	28.5	22.8	51.3	18.6	0.88
	750	36.7	92.2	46.8	30.8	22.4	53.2	19.5	0.89
	800	36.2	94.0	48.2	33.1	18.7	51.8	18.6	0.87
70	600	14.0	32.8	74.0	7.40	18.6	26.0	3.60	0.41
	650	30.4	84.4	57.5	20.2	22.3	42.5	12.9	0.88
	700	36.3	88.2	46.4	29.1	24.5	53.6	19.5	1.05
	750	36.3	92.1	42.6	34.0	23.4	57.4	20.9	1.05
	800	36.0	93.0	45.9	38.2	15.9	54.1	19.5	1.04
95	600	0.0	0.0	—	—	—	—	0.0	—
	650	4.50	14.2	34.2	10.0	55.8	65.8	3.00	0.29
	700	14.8	35.2	26.2	28.5	45.3	73.8	10.9	0.96
	750	36.1	80.1	37.9	41.3	20.8	62.1	22.4	2.35
	800	36.9	91.2	42.8	40.1	17.1	57.2	21.1	2.40

the addition of BaF_2 could enhance the CH_4 conversion as well as the C_2 selectivity of the OCM reaction. Taking the 95 mol% BaF_2/Y_2O_3 catalyst which gave the highest C_2 yield at 750°C as an example, the CH_4 conversion, C_2 selectivity, and C_2 yield were, respectively, 36.1, 62.1, and 22.4%. For pure Y_2O_3, the corresponding values were 30.3, 26.2, and 7.8%. It is apparent that the addition of BaF_2 to Y_2O_3 greatly enhanced the C_2 selectivity and, surprisingly, caused no loss but a gain on CH_4 conversion. Figure 1 shows the variations of CH_4 conversion, C_2 selectivity, and C_2 yield at 750 and 800°C over the BaF_2/Y_2O_3 catalysts with BaF_2 composition ranging from 0 to 100 mol%. The C_2 selectivities over 95 mol% BaF_2/Y_2O_3 and BaF_2 were rather similar, but there was a large drop in CH_4 conversion over pure BaF_2, resulting in the curtailment of the C_2 yield. It is clear that a mixture of BaF_2 and Y_2O_3 performed better than pure BaF_2 or Y_2O_3.

Figure 2 shows the life study of the 95 mol% BaF_2/Y_2O_3 catalyst at 750°C. After 4 h of reaction time, CH_4 conversion started to drop whereas C_2 selectivity began to rise. At 15 h reaction time, the performance of the catalyst appeared to stabilize at a CH_4 conversion of ca. 17% and C_2 selectivity of 73%. The C_2 yield was ca. 13%. After 42 h, the values for CH_4 conversion, C_2 selectivity, and C_2 yield were 16.3, 75.3, and 12.2%, respectively. The C_2H_4/C_2H_6 ratio reduced from ca. 2.0 to 1.2 in the first 8 h and stayed at ca. 1.0 thereafter. According to the results of F^- content analysis, the original F^- content of the catalyst was 21.3 wt%. After 8 h of reaction time, it became 20.2 wt% and after 42 h, it was 19.7 wt%.

Figure 3 shows the variations in specific surface area of the Y_2O_3 and BaF_2/Y_2O_3 catalysts. Generally speaking, the addition of BaF_2 would result in the diminution of specific surface area. The specific surface area of pure Y_2O_3 was 10.5 m^2 g^{-1} and dropped to 3.8 m^2 g^{-1} when 10 mol% of BaF_2 was added. After OCM reactions at 800°C, we found that the catalysts had lost ca. 50% in specific surface area, presumably due to sintering of the catalysts.

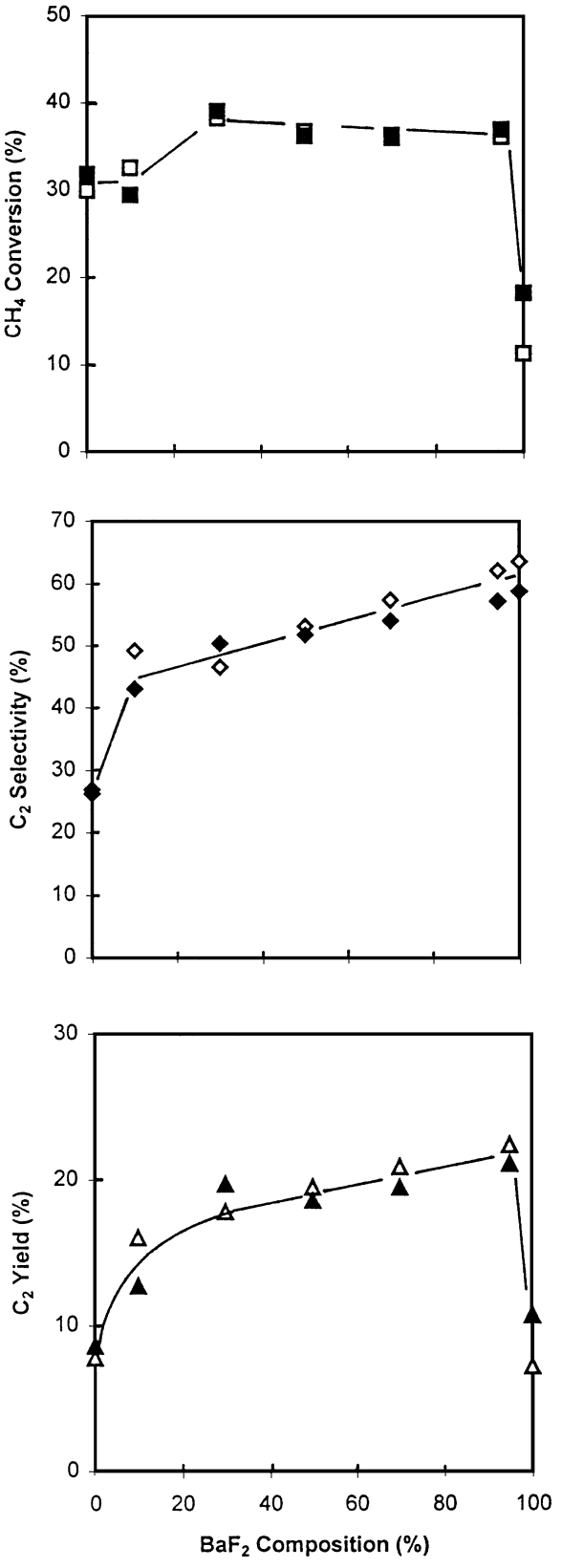

FIG. 1. The catalytic performance at 750 and 800°C of the Y_2O_3 and BaF_2/Y_2O_3 catalysts related to BaF_2 composition (hollow and solid signs denote data at 750 and 800°C, respectively.)

XRD and XPS Studies

Only the BaF_2 and Y_2O_3 crystal phases were observed by XRD investigation in the BaF_2/Y_2O_3 catalysts before and after the OCM reaction (Fig. 4a). According to the XRD pattern, the BaF_2 used in this study has the fluorite structure. Figure 4b clearly illustrates that as BaF_2 was mixed with Y_2O_3, the cubic Y_2O_3 crystal lattice expanded and the cubic BaF_2 crystal lattice contracted. For 0 to 95 mol% BaF_2 compositions, the Y_2O_3 lattice expanded from 10.604 to 10.623 Å. The BaF_2 lattice contracted from 6.200 to 6.188 Å as the Y_2O_3 composition was varied from 0 to 90 mol%. Such distortions increased further during the OCM reaction. The results indicate that some Ba^{2+} ions (radius, 1.43 Å) went into the Y_2O_3 lattice and replaced a certain amount of Y^{3+} ions (radius, 0.88 Å). The larger size of the Ba^{2+} ions and the small coulombic force they induced would result in the expansion of the Y_2O_3 lattice. A certain number of F^- ions might have entered the Y_2O_3 lattice as well. In the BaF_2 lattice, it was the Y^{3+} and O^{2-} ions which were replacing, respectively, the Ba^{2+} and F^- ions and as a result the lattice structure of cubic BaF_2 contracted.

The Y 3*d*, Ba 3*d*, and F 1*s* spectra of the Y_2O_3, 30 mol% BaF_2/Y_2O_3, and 95 mol% BaF_2/Y_2O_3 catalysts are shown in Fig. 5. The Y 3*d* peaks of Y_2O_3 were at 157.8 and 156.1 eV. When BaF_2 was added, the Y 3*d* signals appeared as a broad peak centered at ca. 156.8 eV, indicating that the yttrium ions were perturbed by the presence of Ba^{2+} and F^- ions. The Ba 3*d* and F 1*s* signals were at ca. 779.4 and 683.6 eV, respectively. The surface elemental compositions of the Y_2O_3 and BaF_2/Y_2O_3 catalysts are shown in Table 2. For the Y_2O_3 catalyst, the surface compositions measured before and after the OCM reaction varied only very slightly. For the fresh 30 mol% BaF_2/Y_2O_3 catalyst, the surface Ba/Y ratio was 0.86 and the F/Y ratio was 1.40. For homogeneous distribution of BaF_2 in Y_2O_3, the Ba/Y and F/Y ratios should be 0.21 and 0.43, respectively. Since we have higher values of Ba/Y

TABLE 2

The Elemental Compositon of the Y_2O_3 and BaF_2/Y_2O_3 Catalyst before and after OCM Reactions Based on XPS Results

Catalyst	C 1*s*	Ba 3*d*	O 1*s*	F 1*s*	Y 3*d*	Ba/Y	F/Y	F/Ba
Y_2O_3 (before)	12.3	—	59.7	—	28.0	—	—	—
Y_2O_3 (after)	14.7	—	57.8	—	27.4	—	—	—
30 mol% BaF_2/Y_2O_3 (before)	17.7	16.0	21.5	26.3	18.5	0.86	1.40	1.64
30 mol% BaF_2/Y_2O_3 (after)	17.6	14.6	28.1	20.6	19.1	0.76	1.10	1.41
95 mol% BaF_2/Y_2O_3 (before)	16.8	23.2	13.3	43.0	3.60	6.40	11.9	1.85
95 mol% BaF_2/Y_2O_3 (after)	15.7	19.9	21.2	30.0	13.2	1.50	2.30	1.51

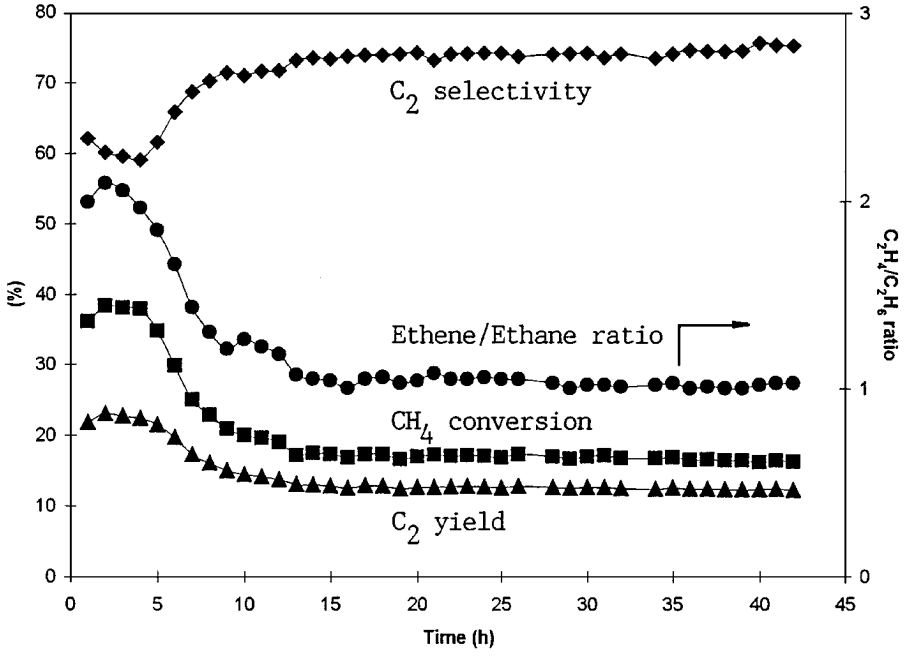

FIG. 2. Life study of the 95 mol% BaF_2/Y_2O_3 catalyst at 750°C.

and F/Y, we conclude that there was BaF_2 accumulated on the surface of Y_2O_3. After the OCM reaction, the values for Ba/Y, F/Y, and F/Ba reduced to 0.76, 1.10, and 1.41, respectively. The results suggest that infiltrations of Ba^{2+} and F^- ions into the Y_2O_3 lattice had occurred. As for the 95 mol% BaF_2/Y_2O_3 catalyst, for homogeneous distribution of Y_2O_3 in BaF_2, the Ba/Y, F/Y, and F/Ba ratios should be 9.5, 19, and 2, respectively. They were 6.4, 11.9, and 1.85 instead for the fresh catalyst and were 1.50, 2.30, and 1.51 after the OCM reaction. In other words, there was enrichment of yttrium on the surface of the catalyst, especially after the OCM reaction.

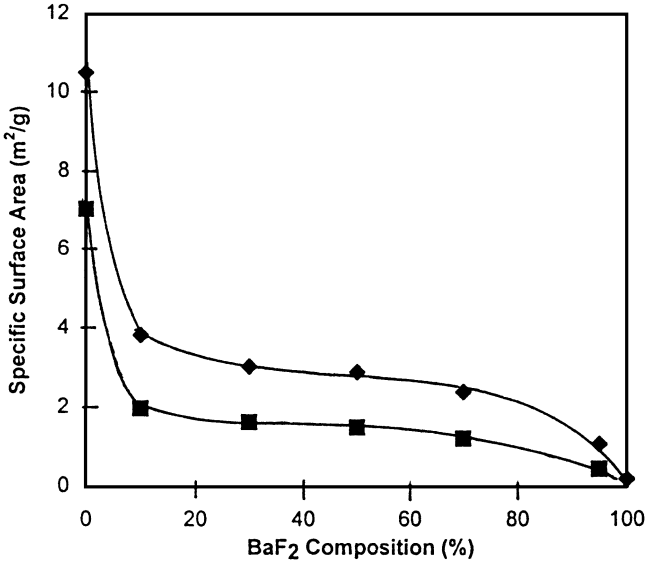

FIG. 3. The changes in specific surface area of the BaF_2/Y_2O_3 catalysts related to BaF_2 composition (◆ bfore and ■ after OCM reactions).

TPR and Raman Studies

Figure 6 shows the TPR spectra of the Y_2O_3, 30 mol% BaF_2/Y_2O_3, and 95 mol% BaF_2/Y_2O_3 catalysts. For Y_2O_3, a TPR band of weak intensity was observed stretching from 300 to 600°C. For the 30 mol% BaF_2/Y_2O_3 catalyst, reduction occurred at ca. 360°C and continued well above 800°C. For the 95 mol% BaF_2/Y_2O_3 catalyst, reduction started at 500°C and carried on above 800°C. After OCM reactions, the amount of reducible oxygen in the 30 mol% BaF_2/Y_2O_3 and the 95 mol% BaF_2/Y_2O_3 catalysts increased considerably and reduction was still occurring at and above 800°C. The results show that there were reducible oxygen species in Y_2O_3. With the addition of BaF_2 to Y_2O_3, the temperature for oxygen reduction to occur shifted to the temperature range (>600°C) suitable for the OCM reaction. Also, the increased amount of reducible oxygen in the 30 mol% BaF_2/Y_2O_3 and 95 mol% BaF_2/Y_2O_3 catalysts used in OCM reactions implies that more sites which could activate O_2 had been generated during the OCM reactions. It is possible that the extents of ionic exchanges between the BaF_2 and Y_2O_3 lattices were augmented during the OCM reaction and more defect sites were generated as a result. The suggestion is supported by the fact that the Y_2O_3 and BaF_2 lattices in the BaF_2/Y_2O_3 catalysts underwent further deformation during the OCM reaction (Fig. 4b).

Figure 7 shows the Raman spectra of the Y_2O_3, 30 mol% BaF_2/Y_2O_3, and 95 mol% BaF_2/Y_2O_3 samples after the

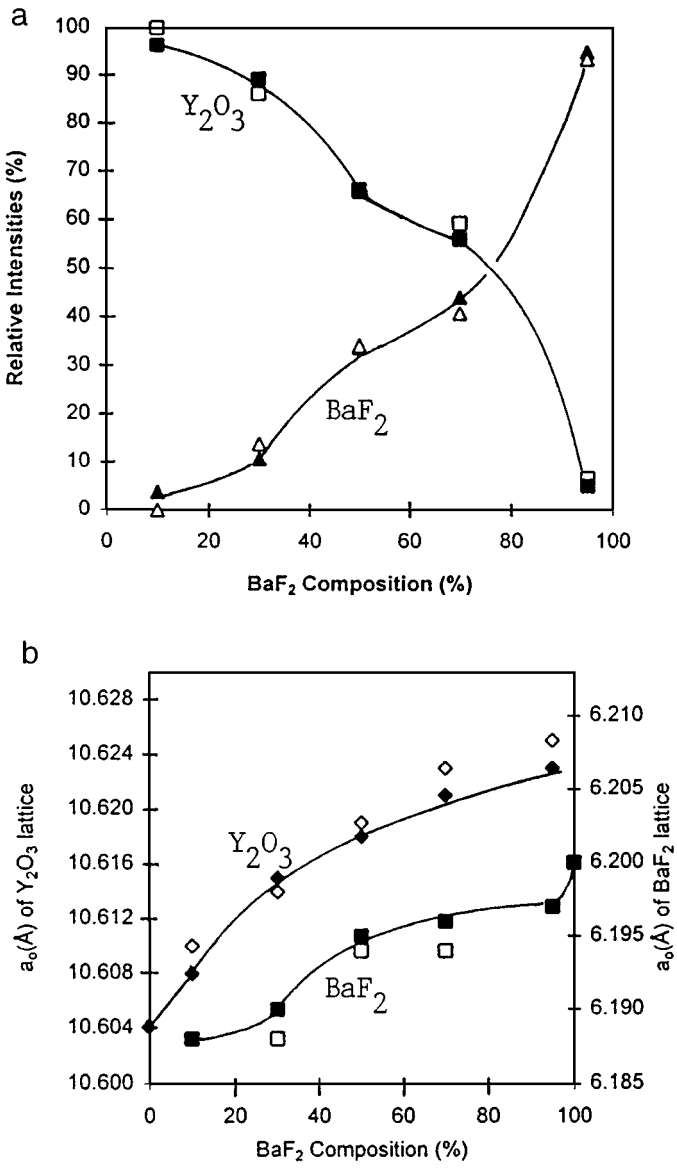

FIG. 4. (a) Phase composition of the BaF_2/Y_2O_3 catalysts related to BaF_2 composition. (■) Y_2O_3, (▲) BaF_2 (hollow signs denote data obtained after OCM reactions), (b) the changes in a_o values of cubic BaF_2 (■) and Y_2O_3 (◆) lattices related to BaF_2 composition (hollow signs denote data obtained after OCM reactions).

samples were exposed to O_2 at 800°C for 15 min and cooled to RT in O_2. The Y_2O_3 sample showed weak Raman bands of good resolution at 1017, 1084, 1104, 1131, 1158, and 1178 cm^{-1}. These could be assigned to the O–O stretching frequencies of various O_2^- species (19). For the 30 mol% BaF_2/Y_2O_3 sample, a broad band centered at 965 cm^{-1} and a weak band at 1313 cm^{-1} were observed. They could be due to, respectively, the O_2^{n-} $(1 < n < 2)$ and $O_2^{\delta-}$ $(0 < \delta < 1)$ species (19). For the 95 mol% BaF_2/Y_2O_3 sample, strong bands centered at 976 and 1319 cm^{-1} due to similar dioxygen species were observed. It is obvious that there were more dioxygen species in 30 mol% BaF_2/Y_2O_3 and 95 mol% BaF_2/Y_2O_3 than in Y_2O_3, especially at high temperatures. One, however, should not draw direct comparison between the TPR and Raman results. The former reflects the amount of oxygen reducible within the recorded range of temperature, while the latter reveals the existence of dioxygen species which are detectable by Raman spectroscopy. There could be mono-oxygen species which were reducible but not detectable by the Raman method.

EPR Studies

After the 95 mol% BaF_2/Y_2O_3 sample was heated in O_2 at 700°C for 10 min and cooled to 25°C in O_2, an EPR signal centered at $g = 2.0079$ with fine structures was observed (Fig. 8a). Treating the sample at 300°C in H_2 for 15 min followed by cooling to 25°C in H_2 caused no major change in spectrum feature but a ca. 12% reduction in signal intensity (Fig. 8b). Heating the sample at 500°C in H_2 for 15 min could result in the generation of a complex EPR signal centered at $g = 2.0871$ (Fig. 8c). Another 30 min in H_2 at 500°C would cause the 2.0871 signal to change from a fairly complex structure to a discrete doublet superhyperfine structure with splittings (Fig. 8d). Reducing (H_2, 15 min) the sample at 600°C would diminish the intensity of the doublet superhyperfine structure (Fig. 8e). After H_2 reduction (15 min) at 700°C, the doublet superhyperfine structure disappeared completely but the 2.0871 signal remained (Fig. 8f). Reduction in H_2 at 750°C for 60 min could generate a new symmetrical signal at 2.0087 with a linewidth of 28 G (Fig. 9a). An EPR signal with similar features has been observed at liquid N_2 temperature over ZnO powder that has been fired in air at 900°C (20). It was suggested that this is due to trapped electrons located in oxygen vacancies.

As shown in Fig. 9a, H_2 reduction (1 h) of a 95 mol% BaF_2/Y_2O_3 sample at 750°C could result in an EPR spectrum with signals at 2.0871 and 2.0087. The former resembled the 2.0871 signal of Fig. 8f, while the latter was a new symmetrical signal with no fine structures. The 2.0087 signal disappeared under paramagnetic O_2, while the signal intensity at 2.0871 was reduced by ca. 15% (Fig. 9b). When purged with N_2 at 25°C, the 2.0087 signal reappeared but with less (by ca. 32%) intensity (Fig. 9c). After another 17 h in O_2 at 25°C followed by purging with N_2 (Fig. 9d), the intensity of the signal at 2.0871 decreased by ca. 36% while that at 2.0087 decreased by ca. 65% compared to Fig. 9a. Heating the sample in O_2 at 200, 300, and 400°C could diminish the signals at 2.0871 and 2.0087 (Figs. 9e–9g). Treatments above 400°C in O_2 would result in the development of an EPR signal centered at 2.0079 with superhyperfine structures (Figs. 9h–9l).

O_2-Pulsing Studies

The 95 mol% BaF_2/Y_2O_3 sample (0.8 g) was first reduced in H_2 at 750°C for 1 h followed by cooling in a flow

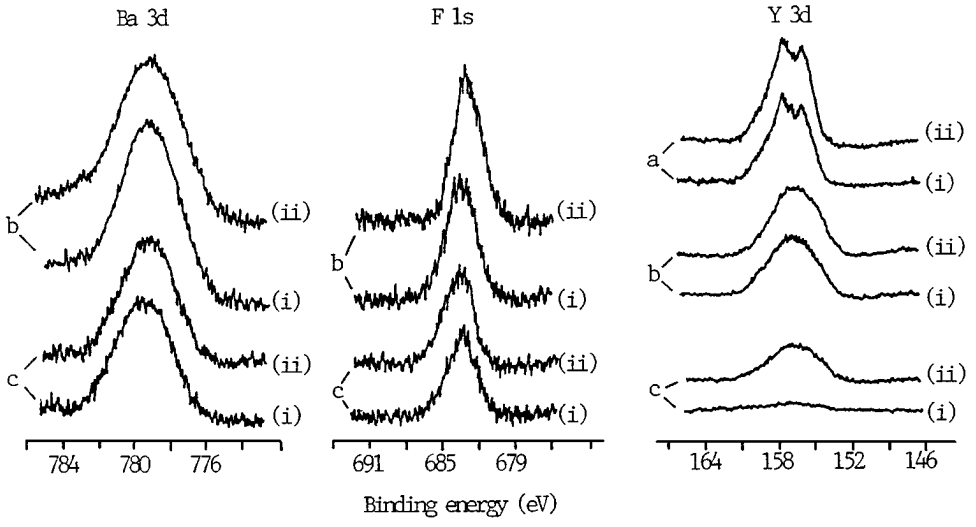

FIG. 5. Ba 3*d*, F 1*s*, and Y 3*d* spectra of the (a) Y_2O_3, (b) 30 mol% BaF_2/Y_2O_3, and (c) 95 mol% BaF_2/Y_2O_3 catalysts before (i) and after (ii) the OCM reaction.

of helium to the desired temperature for O_2 pulsing. We continued to pulse O_2 over the reduced sample until after passing the catalyst, there was no observable decrease in O_2-pulse size. Table 3 shows the amount of O_2 absorbed at various temperatures. In Table 4, an O_2-treated (800°C, 20 min; followed by cooling in O_2 to 25°C and helium purging at 25°C) sample was reduced by H_2 (1 h, followed by He purging for 20 min) at the desired temperature. The O_2 pulsing was performed at 700°C. The experiments were designed with the aim to explore the amount of reducible oxygen ions in the sample and the reactivity of trapped electrons with O_2 at various temperatures. The viewpoint was based on the fact that oxygen ions removed in H_2 reduction were active with H_2 at that temperature, and the amount of O_2 absorbed at 700°C would reflect the amount of oxygen removed. Using the data in Tables 3 and 4, we obtained Arrhenius plots

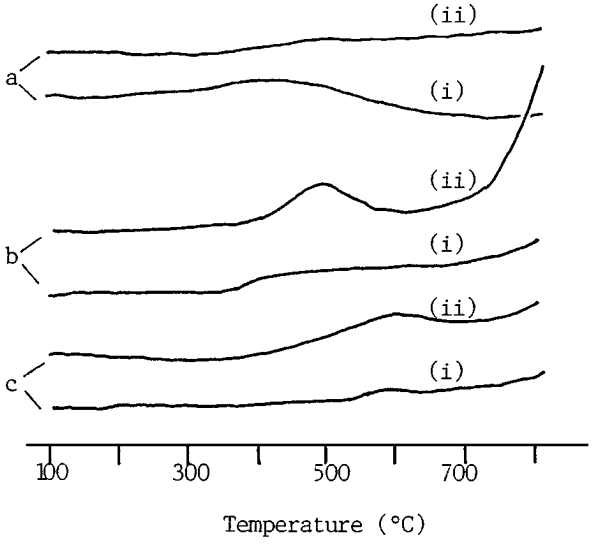

FIG. 6. TPR spectra of the (a) Y_2O_3, (b) 30 mol% BaF_2/Y_2O_3, and (c) 95 mol% BaF_2/Y_2O_3 catalysts before (i) and after (ii) the OCM reaction.

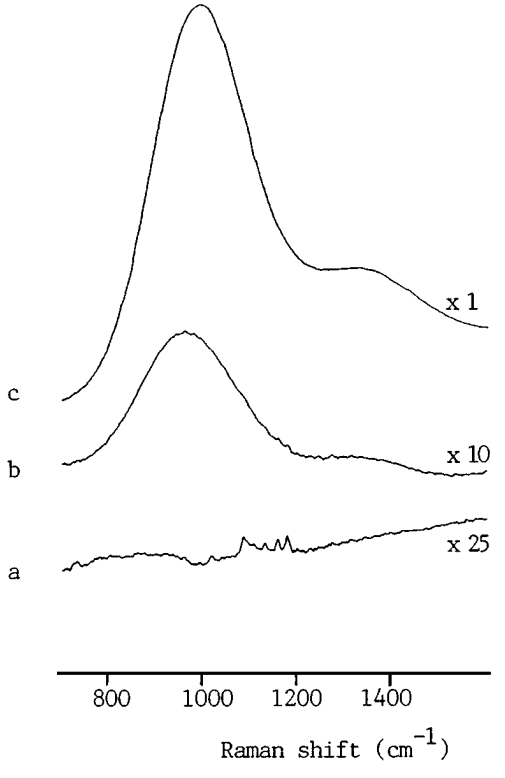

FIG. 7. Raman spectra of the (a) Y_2O_3, (b) 30 mol% BaF_2/Y_2O_3, and (c) 95 mol% BaF_2/Y_2O_3 catalysts after exposures to oxygen.

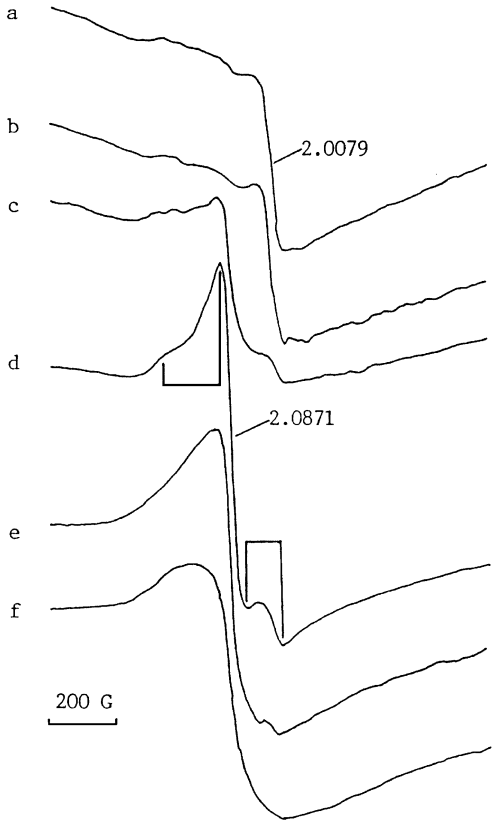

FIG. 8. EPR spectra of 95 mol% BaF_2/Y_2O_3 when it was: (a) heated in O_2 at 700°C for 10 min and cooled to 25°C in O_2; (b) then heated in H_2 at 300°C for 15 min and cooled to 25°C in H_2; (c) then heated in H_2 at 500°C for 15 min and cooled to 25°C in H_2; (d) then heated in H_2 at 500°C for another 30 min and cooled to 25°C in H_2; (e) then heated in H_2 at 600°C for 15 min and cooled to 25°C in H_2; (f) then heated in H_2 at 700°C for 15 min and cooled to 25°C in H_2.

which showed that the activation energy for O_2 interaction with the trapped electrons was 15 ± 4 kJ mol^{-1}. The activation energy for the reduction of oxygen ions by H_2 was around 15 kJ mol^{-1} above 500°C; below 500°C, it was 67 ± 10 kJ mol^{-1}.

TABLE 3

The Amount of O_2 ($\times 10^{-5}$ mol g^{-1}) Absorbed during O_2 Pulsing at Various Sample Temperatures over a H_2-Reduced (750°C, 1 h) 95 mol% BaF_2/Y_2O_3 Sample

O_2 pulsing temperature (°C)	Amount of O_2 absorbed
25	~0
300	0.59
400	0.86
500	2.02
600	2.00
700	2.77
750	3.19

DISCUSSION

From the performances (Table 1 and Fig. 1) of the BaF_2, Y_2O_3, and BaF_2/Y_2O_3 catalysts, one can see that mixing BaF_2 with Y_2O_3 could produce catalysts of good activity for the OCM reaction. The 95 mol% BaF_2/Y_2O_3 catalyst could give a C_2 yield of ca. 22% within the first 4 h of reaction at 750°C. After the fourth hour, CH_4 conversion began to decrease and C_2 selectivity began to rise. After 42 h, the C_2 yield diminished to 12.2%, which was rather low; the C_2 selectivity, however, rose to a respectable value of 75.3%. The C_2H_4/C_2H_6 ratio decreased from ca. 2.0 to 1.0 during

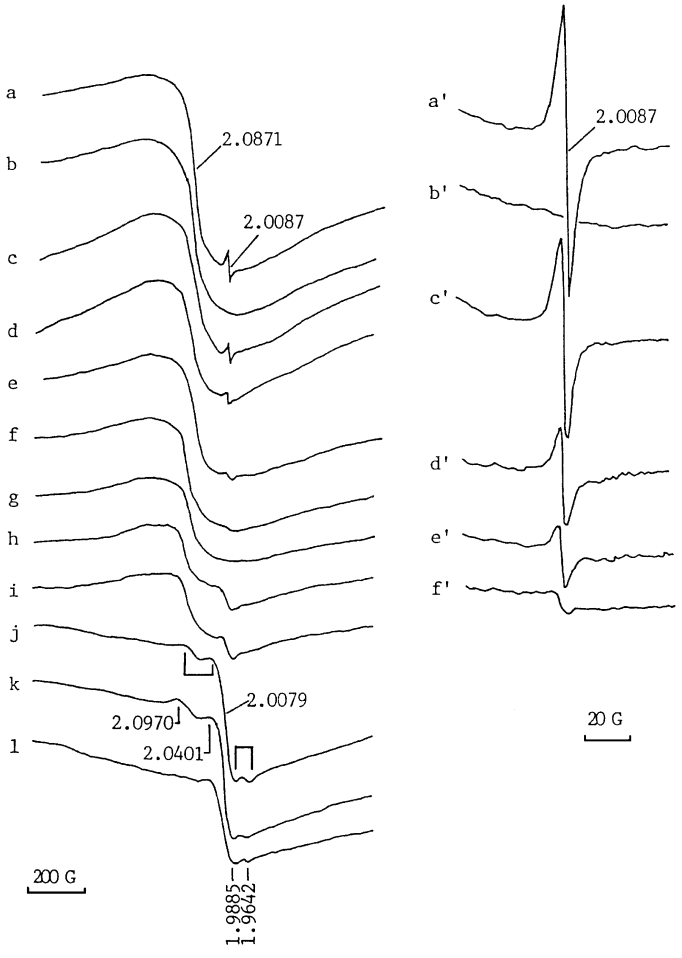

FIG. 9. EPR spectra of an O_2-treated (700°C, 10 min) 95 mol% BaF_2/Y_2O_3 sample when it was: (a) heated in H_2 at 750°C for 60 min and cooled to 25°C in N_2; (b) then under O_2 (10 min) at 25°C; (c) then purged with N_2 at 25°C; (d) then under O_2 for 17 h at 25°C followed by N_2 purging (10 min) at 25°C; (e) then heated in O_2 at 200°C for 10 min and cooled to 25°C in N_2; (f) then heated in O_2 at 300°C for 10 min and cooled to 25°C in N_2; (g) then heated in O_2 at 400°C for 10 min and cooled to 25°C in N_2; (h) then heated in O_2 at 500°C for 15 min and cooled to 25°C in O_2; (i) then N_2-purged for 10 min at 25°C; (j) then heated in O_2 at 600°C for 15 min and cooled to 25°C in O_2; (k) then N_2-purged for 10 min at 25°C; (l) then heated in O_2 at 700°C for 15 min and cooled to 25°C in O_2 (a′ to f′ are the enlarged signals at 2.0087 corresponding to spectra a to f).

TABLE 4

The Amount of O_2 ($\times 10^{-5}$ mol g^{-1}) Absorbed during O_2 Pulsing at 700°C over an O_2-Treated 95 mol% BaF_2/Y_2O_3 Sample H_2 Reduced (1 h) at Various Temperatures

H_2 reduction temperature (°C)	Amount of O_2 absorbed
25	~0
100	~0
200	~0
300	0.18
400	0.49
450	1.54
500	1.78
550	2.10
600	2.52
700	2.72
750	2.77

the 42 h of the OCM reaction, possibly due to the leaching of fluorine. The BET results in Fig. 3 clearly illustrate that the specific surface areas of the catalysts had decreased, possibly due to surface sintering, during the OCM reaction. According to the heterogeneous–homogeneous reaction scheme referred to by Lin *et al.* (21), Iwamatsu *et al.* (22), and ourselves (23), the diminution in specific surface area would enhance C_2 selectivity and diminish CH_4 conversion. Such a scheme can explain what was happening during the life study of the 95 mol% BaF_2/Y_2O_3 catalyst. As the catalyst sintered, the surface area diminished and the CH_4 conversion decreased from ca. 38 to 16% while the C_2 selectivity increased from ca. 60 to 75%.

According to Fig. 3, the increase in BaF_2 composition would cause the specific surface area of the BaF_2/Y_2O_3 catalysts to decrease as well. However, although we could see an increase in C_2 selectivity with the increase in BaF_2 content, we did not see any drop in CH_4 conversion. As a matter of fact, the CH_4 conversion increased (Fig. 1). It is apparent that the heterogeneous–homogeneous scheme mentioned earlier fails here. Other determining factor(s) must be working to counteract the effects caused by the diminution of specific surface area. A plausible explanation is that the mixing of BaF_2 with Y_2O_3 created defects that could promote the activation of O_2 and in return enhanced the CH_4 conversion. The TPR (Fig. 6) and Raman (Fig. 7) results clearly indicate that the BaF_2/Y_2O_3 catalysts were more capable of activating O_2 than Y_2O_3. In the XRD studies, we observed an expanded cubic Y_2O_3 and a contracted cubic BaF_2 phase in the 95 mol% BaF_2/Y_2O_3 sample. Such contraction could only be caused by the infiltrations of Y^{3+} and O^{2-} ions into the BaF_2 lattice. As suggested before (17), these types of ionic substitutions could lead to the formation of defects such as anion vacancies, O^- ions, and trapped electrons. Based on the XRD results, the BaF_2 used in this study has the fluorite structure. According to Wells (24), Y_2O_3 adopts the *C*-M_2O_3 structure which is related to the fluorite structure "by removing one-quarter of the anions and then rearranging the atoms somewhat." Given these strong structural similarities, it is quite plausible that the two phases might have doped each other, resulting in the rather complex intergrowth chemistry. In Fig. 8, since the sample had been treated in O_2 at 700°C (10 min) and cooled in O_2 to 25°C, the EPR signal centered at 2.0079 is likely to be caused by oxygen ions. Y^{3+} ions are not paramagnetic (with a Kr core) and will not broaden the EPR signals of nearby paramagnetic species. However, it is known that dipolar interaction between gas-phase and surface paramagnetic species can broaden the EPR signal of surface paramagnetic species, rendering the surface paramagnetic species EPR-undetectable (17). Hence the species detected in Fig. 8a were in the bulk of the 95 mol% BaF_2/Y_2O_3 sample. Heating the oxidized sample at or above 300°C in H_2 would result in the removal of oxygen from the sample (Table 3). This was reflected in the change of EPR signals. Reduction at 300°C would cause spectrum 8a to decrease by ca. 15% in intensity, indicating the removal of oxygen ions in the sample,

$$O_2^{2-} + H_2 \rightarrow 2OH^-$$
$$O_2^- + H_2 \rightarrow O_2H^- + H\cdot$$
$$O_2H^- + H\cdot \rightarrow O^- + H_2O\uparrow + [\,]$$
$$O^- + H_2 \rightarrow OH^- + H\cdot$$
$$O^{2-} + H\cdot \rightarrow OH^- + [e^-]$$
$$OH^- + H\cdot \rightarrow H_2O\uparrow + [e^-],$$

where [ ] denotes an anion vacancy and $[e^-]$ a trapped electron. From the above interactions of H_2 with oxygen ions, one can see that $H\cdot$ and $[e^-]$ could be generated. The interaction of $H\cdot$ with O^{2-} ion could also generate trapped electrons as suggested by Tench *et al.* (25).

The reduction of the sample by H_2 above 500°C was a rather facile process and the activation energy for the reaction was estimated to be about 15 kJ mol^{-1}. Between 300 and 500°C, it was around 67 kJ mol^{-1}. Yttrium and barium might not have been reduced to their metallic states, but the removal of oxygen from the catalyst during H_2 reduction was rather clear. Based on these understandings, we propose that the EPR signals centered at 2.0871 in Figs. 8c–8f were due to trapped electrons. Spectrum 8c shows the transition state of a partially reduced 95 mol% BaF_2/Y_2O_3 sample as the spectrum still bore a certain resemblance to spectrum 8b. The complexity of spectrum 8c was a result of the presence of both oxygen ions and trapped electrons in the sample. After reduction in H_2 at 500°C for a total period of 45 min, more oxygen ions detected in spectrum 8a were removed and spectrum 8d shows a discrete doublet superhyperfine structure. This strong superhyperfine EPR

signal is assigned to trapped electrons interacting with the Y^{3+} ions. However, further reduction in H_2 at temperatures above 500°C would cause such superhyperfine structure to disappear. We propose that due to intense reduction, the population of trapped electrons increased and the interaction among the trapped electrons became significant. The superhyperfine signals were hence broadened and could not be seen. The presence of gaseous O_2 would cause a ca. 15% reduction in intensity of the 2.0871 signal. In other words, ca. 85% of these trapped electrons were in the bulk.

Nevertheless, reduction (1 h) of the 95 mol% BaF_2/Y_2O_3 sample in H_2 at 750°C would generate the EPR signal at 2.0087 (Fig. 9a). We assign this signal to another type of trapped electron. Compared to the trapped electrons with EPR signals centered at 2.0871, this type of trapped electron appeared to be absolutely surface-bound, as the introduction of gaseous O_2 would completely remove the 2.0087 signal (Fig. 9b). We suggest that these trapped electrons were in surface anion vacancies and were shared among the orbitals of the surrounding cations. The relatively low g value could be ascribed to the rather "free" nature of such surface-trapped electrons.

Hence by reducing the 95 mol% BaF_2/Y_2O_3 catalyst in H_2, we could generate two types of trapped electrons. One had the EPR signal centered at 2.0087 located on the surface. The other had the EPR signal centered at 2.0871, located near the Y^{3+} ions and spread throughout the sample. Prolonged exposure (17 h) of the sample to O_2 at 25°C (Fig. 9c) could not eliminate these signals completely. Compared to spectrum 9a, the 2.0871 and 2.0087 intensities in spectrum 9d had reduced roughly by 36 and 65%, respectively. The results imply that the combination of O_2 with trapped electrons to generate oxygen ions had occurred. As shown in Fig. 9, the 2.0087 signal disappeared completely after O_2 treatment at 400°C (spectrum 9g), while the complete disappearance of the 2.0871 signal could be observed only after O_2 treatment at 600°C (spectrum 9j), implying that the complete consumption of the trapped electrons with EPR signals at 2.0087 and 2.0871 occurred, respectively, at 400 and 600°C. In other words, the 2.0871 trapped electrons in the bulk were more stable than the 2.0087 trapped electrons on the surface.

Treatments of the sample in O_2 at and above 500°C would generate the EPR signal centered at 2.0079 (Figs. 9h–9l). After O_2 treatment at 600°C, a strong EPR signal centered at 2.0079 showing superhyperfine structures existed (Fig. 9k). This EPR signal was from the bulk, as the presence of gaseous O_2 did not weaken it. Treatment in O_2 at 700°C would produce EPR spectra that resembled spectrum a of Fig. 8. These spectra resemble the typical outline of O_2^- ions reported by Louis *et al.* (7) and Ito *et al.* (8). In the studies of Y_2O_3–CaO catalysts for the OCM reaction, Osada *et al.* (14) observed EPR signals at 2.070 and 2.040 and assigned them to interstitial O_2^- ions coordinated to Ca^{2+} and Y^{3+}, respectively. Hence we assign the features in the 2.0456 to 2.2500 and 1.9642 to 1.9885 ranges, respectively, to $g_\parallel$ and $g_\perp$ components of O_2^- ions in the bulk. Since we observed doublet superhyperfine structures, we suggest that there were O_2^- ions interacting with the Y^{3+} ions.

Based on the data in Tables 3 and 4, we know that at or above 300°C , O_2 absorption by the H_2-reduced catalyst was remarkable. We observed the complete disappearance of the 2.0087 EPR signal due to surface-trapped electrons and a further decrease in intensity of the 2.0871 signal assigned to trapped electrons close to Y^{3+} (Fig. 9). We conclude that O_2 activation at 400°C involved the total number of the trapped electrons with a signal at 2.0087 and certain portion of the trapped electrons with a signal at 2.0871 (likely to be those on and/or close to the surface). Above 400°C, there was a large increase in the amount of O_2 absorbed (Tables 3 and 4). We believe that at these temperatures, in addition to the trapped electrons on and/or close to the surface, those in the bulk were involved in the activation of O_2. Compared to the trapped electrons generated by UV irradiation over metal oxides, the trapped electrons observed over the 95 mol% BaF_2/Y_2O_3 sample were very stable. The trapped electrons reported by Lunsford *et al.* (5), Yanagisawa *et al.* (26), and Ito *et al.* (27) were on the surface of metal oxides and existed only below −73°C. The trapped electrons in the 95 mol% BaF_2/Y_2O_3 sample were stable because the migration of electrons in a F^- matrix was far more difficult than that in an O^{2-} matrix, as suggested in the case of 20% SrF_2/SmOF (17).

CONCLUSION

The two-component BaF_2/Y_2O_3 catalysts are better catalysts for the OCM reaction than the one-component BaF_2 and Y_2O_3 catalysts. TPR and Raman studies revealed that the BaF_2/Y_2O_3 catalysts are more capable than the undoped Y_2O_3 sample of activating O_2. Based on the results of XRD studies, we are sure that inside the 95 mol% BaF_2/Y_2O_3 catalyst, there were structural defects created in the cubic BaF_2 lattice. Detailed EPR investigations showed that two types of trapped electrons could be generated in the reduction of 95 mol% BaF_2/Y_2O_3. H_2 reduction above 500°C would result in the generation of trapped electrons located close to Y^{3+} ions with an EPR signal centered at 2.0871. H_2 reduction above 700°C would produce trapped electrons with an EPR signal centered at 2.0087. The trapped electrons with an EPR signal at 2.0087 were surface-bound, while those with a signal at 2.0871 existed both on the surface and in the bulk. Trapped electrons on the surfaces were active at 25°C and reacted with O_2 to form dioxygen ions. Above 500°C, the diffusion of oxygen ions became significant and trapped electrons in the bulk were involved in oxygen reduction. Most of the trapped electrons were active

above 500°C and combined with O_2 to form dioxygen ions. There were O_2^- ions close to Y^{3+} ions, as the EPR signals of O_2^- ions showed doublet superhyperfine structures. We suggest that the hydrogen dissociated from methane in the OCM reaction could reduce the BaF_2/Y_2O_3 catalysts, resulting in the generation of trapped electrons. These trapped electrons could serve as active sites for O_2 activation, resulting in the enhancement of CH_4 conversion in the OCM reaction.

ACKNOWLEDGMENTS

The project was supported by the Hong Kong Research Grants Council, UGC (HKBC146/95P). W.J.J. thanks the Croucher Foundation for a visitorship. Y.W.L. thanks the HKBU for a Ph.D. studentship. We thank the Department of Chemistry, Xiamen University, Xiamen, PR China, for the facilitation of the EPR measurements.

REFERENCES

1. Lunsford, J. H. *Catal. Rev.-Sci. Technol.* **8**, 135 (1973).
2. Che, M., and Tench, A. H., *Adv. Catal.* **31**, 78 (1982).
3. Yamashita, H., Machida, Y., and Tomita, A., *Appl. Catal. A: General* **79**, 203 (1991).
4. Nakamura, M., Fujita, S., and Takezawa, N., *Catal. Lett.* **14**, 315 (1992).
5. Lunsford, J. H., and Jayne, J. P., *J. Phys. Chem.* **44**, 1487 (1966).
6. Wong, N. B., and Lunsford, J. H., *J. Chem. Phys.* **56**, 2664 (1972).
7. Louis, C., Chang, T. L., Kermarec, M., Van, T. L., Tatibouet, J. M., and Che, M., *Catal. Today* **13**, 283 (1992).
8. Ito, T., Kato, M., Toi, K., Shirakawa, T., Ikemoto, I., and Tokuda, T., *J. Chem. Soc. Faraday Trans. 1* **81**, 2835 (1985).
9. Wang, J. X., and Lunsford, J. H., *J. Phys. Chem.* **90**, 5883 (1986).
10. Zecchina, A., Lofthouse, M. G., and Stone, F. S., *J. Chem. Soc. Faraday Trans.* **71**, 1476 (1975).
11. Coluccia, S., Deane, A. M., and Tench, A. J., *J. Chem. Soc. Faraday Trans.* **74**, 2913 (1978).
12. Coluccia, S., Boccuzzi, F., Ghiotti, G., and Mirra, C., *Z. Phys. Chem. (N.F.)* **121**, 141 (1980).
13. Cordischi, D., Indovina, V., and Occhiuzzi, M., *J. Chem. Soc. Faraday Trans.* **74**, 456 (1978).
14. Osada, Y., Koike, S., Fukushima, T., Ogasawara, S., Shikada, T., and Ikariya, T., *Appl. Catal.* **59**, 59 (1990).
15. Kaminsky, M. P., Zajac, G. W., Campuzano, J. C., Faiz, M., Beaulaige, L., Gofron, K., Jennings, G., Yao, J. M., and Saldin, D. K., *J. Catal.* **136**, 16 (1992).
16. Erarslanoglu, Y., Onal, I., Dogu, T., and Senkan, S., *Appl. Catal. A* **145**, 75 (1996).
17. Au, C. T., and Zhou, X. P., *J. Chem. Soc. Faraday Trans.* **92**, 1793 (1996).
18. Au, C. T., He, H., Lai, S. Y., and Ng, C. F., *J. Catal.* **159**, 280 (1996).
19. Au, C. T., and Zhou, X. P., *J. Chem. Soc. Faraday Trans.* **93**, 485 (1997).
20. Kasai, P. H., *Phys. Rev.* **30**, 989 (1962).
21. Lin, C. H., Wang, J. X., and Lunsford, J. H., *J. Catal.* **111**, 302 (1988).
22. Iwamatsu, E., Moriyama, T., Takasaki, N., and Aika, K., *J. Catal.* **113**, 25 (1988).
23. Au, C. T., Zhang, Y. Q., Ng, C. F., and Wan, H. L., *Catal. Lett.* **23**, 377 (1994).
24. Wells, A. F., "Structural Inorganic Chemistry, 5th ed.," p. 545. Oxford Univ. Press, Oxford, 1984.
25. Tench, A. J., Lawson, T., and Kibblewhite, J. F. J., *J. Chem. Soc. Faraday Trans.* **68**, 1169 (1972).
26. Yanagisawa, Y., and Hyzimura, R. *J. Phys. Soc. Jpn* **50**, 209 (1981).
27. Ito, T., Watanabe, M., Kogo, K., and Tokuda, T., *Z. Phys. Chem. (N.F.)* **124**, 83 (1981).